Abbreviated title: HISTORY MODULATES DISTRACTORS

History modulates early sensory processing of salient distractors

Kirsten C.S. Adam[1] & John T. Serences[1,2,3]

[1] Department of Psychology, *University of California San Diego*
[2] Institute for Neural Computation, *University of California San Diego*
[3] Neurosciences Graduate Program, *University of California San Diego*

Word count (abstract): 237
Word count (not including abstract, methods, references, figure legends): 5,471
Word count (methods): 2,463
Tables: 0
Figures: 6

Keywords: visual search; fMRI; priority maps; attentional selection; salience

Contributions: K.A. collected data, performed analyses, and drafted the manuscript. Both authors designed the study and revised the manuscript.

Funding: Research was supported by National Eye Institute grant R01 EY025872 (J.S.), National Institute of Mental Health grant T32-MH020002 (K.A.), and National Eye Institute grant T32-EY020503 (K.A.).

Data availability: Data will be made freely available online on the Open Science Framework at https://osf.io/wrdvz/ upon acceptance for publication.

Acknowledgements: We thank Rosanne Rademaker for scanning assistance and for sharing custom analysis code. We thank Nicole Rangan and Matteo d'Amico for assistance with behavioral data collection, and we thank Ed Awh for helpful comments on earlier drafts of the manuscript.

Conflicts of interest: none

Correspondence to:
Kirsten C. S. Adam
University of California San Diego
9500 Gilman Drive, Mail Code: 0109
La Jolla, CA 92093-0109
kadam@ucsd.edu

Abstract

To find important objects, we must focus on our goals, ignore distractions, and take our changing environment into account. This is formalized in models of visual search whereby goal-driven, stimulus-driven and history-driven factors are integrated into a priority map that guides attention. Stimulus history robustly influences where attention is allocated even when the physical stimulus is the same: when a salient distractor is repeated over time, it captures attention less effectively. A key open question is how we come to ignore salient distractors when they are repeated. Goal-driven accounts propose that we use an active, expectation-driven mechanism to attenuate the distractor signal (e.g., predictive coding), whereas stimulus-driven accounts propose that the distractor signal is attenuated due to passive changes to neural activity and inter-item competition (e.g., adaptation). To test these competing accounts, we measured item-specific fMRI responses in human visual cortex during a visual search task where trial history was manipulated (colors unpredictably switched or were repeated). Consistent with a stimulus-driven account of history-based distractor suppression, we found that repeated singleton distractors were suppressed starting in V1, and distractor suppression did not increase in later visual areas. In contrast, we observed signatures of goal-driven target enhancement that were absent in V1, increased across visual areas, and were not modulated by stimulus history. Our data suggest that stimulus history does not alter goal-driven expectations, but rather modulates canonically stimulus-driven sensory responses to contribute to a temporally-integrated representation of priority.

Significance Statement

Visual search refers to our ability to find what we are looking for in a cluttered visual world (e.g., finding your keys). To perform visual search, we must integrate information about our goals (e.g., 'find the red key-chain'), the environment (e.g., salient items capture your attention), and changes to the environment (i.e., stimulus history). Although stimulus history impacts behavior, the neural mechanisms that mediate history-driven effects remain debated. Here, we leveraged fMRI and multivariate analysis techniques to measure history-driven changes to the neural representation of items during visual search. We found that stimulus history influenced the representation of a salient 'pop-out' distractor starting in V1, suggesting that stimulus history operates via modulations in early sensory processing rather than goal-driven expectations.

Introduction

At any moment we can selectively attend only a small fraction of available perceptual inputs, so we need to select a subset of information and discard irrelevant information. This capacity limit poses a significant computational challenge, particularly given that perceptual inputs constantly change as we move through the world. Given our constantly changing surroundings, one particularly useful computational strategy is to discard information that stays the same over time. For example, when searching for sea glass at the beach, irrelevant but salient information (e.g., a red plastic bottle-cap) may grab our attention. But, if we repeatedly encounter the same irrelevant information (e.g., the beach is littered with red bottle-caps), then we can come to ignore initially salient distractors. Extensive evidence suggests that stimulus history robustly modulates behavior: An initially salient color distractor no longer captures our attention after we have seen it many times (Geyer et al., 2006; Vatterott and Vecera, 2012; Geng, 2014; Gaspelin et al., 2015, 2017; Wang and Theeuwes, 2018a; Failing et al., 2019a; Geng et al., 2019; Van Moorselaar and Slagter, 2020). Yet, debate persists as to how this history-driven behavioral modulation is achieved: Do we use an active, expectation-based mechanism to suppress the salient distractor signal when it is repeated (e.g., predictive coding), or, is the distractor signal passively attenuated because of changes to neural activity with repetition (e.g., adaptation)? Here, we leverage item-specific, neural estimates of priority, to test competing hypotheses of how stimulus history alters attentional priority.

Models of visual search hypothesize that we integrate information about what is relevant *(goal-driven* or *'top-down' factors*), what is salient given local image statistics *(stimulus-driven* or *'bottom-up' factors*), and what has occurred in the past (*history-driven factors*) via an integrated, topographically organized "priority map" (Treisman and Gelade, 1980; Wolfe, 1994; Itti and Koch, 2000; Fecteau and Munoz, 2006; Serences and Yantis, 2006; Awh et al., 2012). Note, some work uses the terms 'saliency' and 'priority' interchangeably, whereas other work uses these terms to refer to distinct concepts. Here, we use 'priority' to refer to the integration of goal-driven and stimulus-driven task factors, and 'saliency' to refer to strictly image-computable, stimulus-driven task factors (Serences and Yantis, 2006). Although both stimulus-driven and goal-driven information is

represented to some extent in many cortical regions (Silver et al., 2005; Serences and Yantis, 2006, 2007; Saproo and Serences, 2010; Bogler et al., 2011; Sprague and Serences, 2013; Sprague et al., 2018b), areas of parietal cortex (e.g., LIP, IPS) are hypothesized to be ideal candidates for integrating information about stimulus-driven sensory inputs from occipital cortex and information about goals from pre-frontal cortex (Ipata et al., 2006, 2009; Bisley and Mirpour, 2019; Theeuwes, 2019).

History-driven effects have only recently been added to models of visual search, in part because these effects do not wholly fit within a 'goal-driven' versus 'stimulus-driven' dichotomous framework (Awh et al., 2012; Geng, 2014; Le Pelley et al., 2016; Geng et al., 2019; Van Moorselaar and Slagter, 2020). Rather, history-driven effects rely on both current sensory input and prior experiences. Thus, debate persists about whether stimulus history influences attentional priority by co-opting elements of stimulus-driven computations, goal-driven computations, or another pathway altogether (Gaspelin et al., 2015; Gaspelin and Luck, 2018; Wang and Theeuwes, 2018b; Geng et al., 2019; Theeuwes, 2019; Van Moorselaar and Slagter, 2020).

Goal-driven accounts propose that we exploit voluntary selection mechanisms to incorporate information about history-driven task factors into priority maps. Earlier work has shown how voluntary attention may be used to enhance the target item relative to the other distractor items: when looking for a particular target, one may form a "template" of that feature and use this template to voluntarily up-regulate relevant portions of the visual field (Pashler and Shiu, 1999; Downing, 2000; Soto et al., 2005; Olivers et al., 2006; Carlisle et al., 2011; Beck et al., 2012). Similar voluntary selection mechanisms might likewise be used to suppress a distractor signal when it is repeated, either directly or indirectly. First, distractor suppression could arise *indirectly* because of predictive coding and biased competition (Desimone and Duncan, 1995; Spratling, 2008; Summerfield and de Lange, 2014). In this account of history-driven distractor suppression, participants could use their expectations about the upcoming, repeated stimulus futures to more strongly enhance the target and, consequently, the competing distractor would be automatically suppressed due to inter-item competition (Spratling, 2008). Second, distractor suppression could arise *directly*, via a top-down suppression signal for a

specific feature. This direct suppression signal is sometimes referred to as a "negative search template" (Arita et al., 2012; Moher and Egeth, 2012; Reeder et al., 2017; Conci et al., 2019, but see: Beck and Hollingworth, 2015; Becker et al., 2015). Critically, in either the direct or indirect case, we would expect to observe a similar neural signature at the level of population codes measured with fMRI for both of these goal-driven accounts. Specifically, we should observe that distractor suppression effects are greater in later visual areas (e.g., IPS0) than in earlier visual areas (e.g., V1), consistent with a goal-driven signal (e.g., Silver et al., 2005; Sprague et al., 2018b). In the case of the predictive coding / biased competition model (Spratling, 2008), we would further predict that target enhancement and distractor suppression should be yoked, whereby greater distractor suppression will be accompanied by greater target enhancement as arrays are repeated.

In contrast, stimulus-driven accounts instead suggest that history-driven distractor suppression can arise from passive changes to neural activity as stimuli are presented over time (Turatto and Pascucci, 2016; Turatto et al., 2018; Wang and Theeuwes, 2018a; Failing et al., 2019a; Won and Geng, 2020). For example, some work suggests that even passive, task-irrelevant exposure to a particular feature may be sufficient to alter attentional guidance and search behaviors (Engel and Furmanski, 2001; Grill-Spector and Malach, 2001; Gardner et al., 2005; Kristjansson et al., 2007; Turatto and Pascucci, 2016; Turatto et al., 2018; Won and Geng, 2020). Although the effects of adaptation for single stimuli are well understood, how adaptation affects saliency in multi-item displays has only recently been considered. Yet, emerging evidence suggests that altered firing rates from simple sensory adaptation effects could alter inter-item competition (Solomon and Kohn, 2014) which, in turn, could alter stimulus saliency and behavior (Treisman and Gelade, 1980; Wolfe, 1994; Itti and Koch, 2000; Li, 2002; Zhang et al., 2012).

Here, we tackle the debate about history-driven distractor suppression from a new angle: we measured neural activity via fMRI in human subjects performing a visual search task in order to estimate item-specific changes to neural priority across the visual stream. Critically, we manipulated trial history so that we could compare neural responses to physically identical displays (e.g., green target, red singleton distractor) as a function of trial history (i.e., whether the colors of preceding displays repeated or varied).

Materials and Methods

Participants

Experiment 1a: MRI experiment. Healthy volunteers (*n* = 12; 9 female; mean age = 25.3 years [SD = 2.5, min = 21, max = 30]; all right-handed; normal or corrected-to-normal visual acuity; normal color vision) participated in three ~2 hour sessions at the Keck Center for fMRI on the University of California San Diego (UCSD) campus, and were compensated $20/hr. Procedures were approved by the UCSD Institutional Review Board, and participants provided written informed consent. Sample size was determined by a power analysis on data from Sprague et al.(Sprague et al., 2018b) where achieved power (1-ß) to detect a within-subjects attention modulation using an inverted encoding model was 83% (across 10 ROIs) with n=8. We planned for n =11 to achieve estimated 90% power (rounded up to n = 12 to satisfy our counter-balancing criteria).

Experiment 1b: Behavior only. Healthy volunteers (*n* = 24; 21 female; mean age = 19.8 years [SD = 1.5, min = 18, max = 24]; normal or corrected-to-normal visual acuity; normal color vision; handedness not recorded) participated in one 1.5-hour experimental session in the Department of Psychology on the UCSD campus, and were compensated with course credit. There were no duplicate participants across experiments. Procedures were approved by the UCSD IRB, and all participants provided written informed consent. A sample size of 24 was chosen *a priori* based on published papers(Gaspelin et al., 2015).

Session procedures

Exp 1a, Retinotopy session. Participants completed one retinotopic mapping session prior to participation in the experimental sessions, following standard procedures(Engel et al., 1994; Swisher et al., 2007). Some participants had already completed a retinotopy session as part of prior studies in the lab; this session was used if available. Retinotopy data were used to identify retinotopic ROIs (V1-V3, V3AB, hV4, VO1, VO2, LO1, LO2, TO1, TO2, IPS0-4). During each session, participants viewed flickering checkerboards. On meridian mapping runs, a “bowtie” checkerboard alternated between the horizontal and vertical meridians. On polar angle mapping runs, a checkerboard wedge slowly rotated in a clockwise or counterclockwise direction. On

eccentricity mapping runs, a "donut" checkerboard began near fixation and its radius slowly expanded outward. A high-resolution anatomical scan was collected for functional alignment. Anatomical and functional retinotopy analyses were performed using custom code calling existing FreeSurfer and FSL functions. Functional retinotopy data were used to draw ROIs, but only voxels that were also visually responsive to experimental localizers (below) were analyzed further.

Exp 1a, Main MRI session. Participants completed two experimental sessions. In each session, they completed 2 runs of the item position localizer, 4 runs of the spatial location localizer, and 8 runs of the search task (4 runs "color variable", 4 runs "color constant"). When time allowed, extra localizer runs were collected. Some participants also took part in an unrelated study in which additional localizers were collected. Across the two sessions, participants completed 16 runs of visual search (M = 1,1152 trials, SD = 0), an average of 11.2 runs of the spatial location localizer (M = 1,072 trials, SD = 298, min = 768, max = 1,536), and an average of 4.3 item position localizer runs (M = 381 trials, SD = 43, min = 352, max = 440).

Exp 1b. Participants completed 12 blocks of the search task (6 blocks "color variable", 6 blocks "color constant").

Stimuli and task procedures

Experiment 1a: MRI

Stimuli were projected on a 21.5 x 16 cm screen mounted inside the scanner bore. The screen was viewed from a distance of ~47 cm through a mirror. Stimuli were generated in MATLAB (2017b, The MathWorks, Natick, MA) with the Psychophysics toolbox (Brainard, 1997; Pelli, 1997) on a laptop running Ubuntu. Responses were collected with a 4-button button box. Stimuli for each task are shown in Figure 1.

Item position localizer. Participants viewed reversing checkerboards (4 Hz flicker) which occupied the locations of the items in the search task (each item radius = 2.5º placed on an imaginary circle 7º from fixation, with one item in each of the 4 quadrants on the circle). Participants were shown items on 2 alternating diagonals (i.e., items in Quadrants 1 and 3 and then Quadrants 2 and 4) for 3 sec each. There were 88

stimulus presentations within each run. Participants were instructed to attend to both items, and to press a button if either item briefly dimmed. A brief (250 ms) dimming occurred on 1 of the 2 items for 25% of stimulus presentations.

Spatial location localizer. Participants viewed a reversing checkerboard wedge (flicker = 4 Hz; white & black checkerboards) at one of 24 positions. Checkerboard positions were equally spaced along a circle with radius = 7º, and wedges were non-overlapping (i.e., each wedge's width along the circle filled a 15º arc and was ~5º of visual angle in height). The wedge stayed at one position for 3 sec, then moved to a different position (with the constraint that back-to-back positions must be in different quadrants). There were 96 wedge presentations within each run. Participants were instructed to attend to the fixation point; if the fixation point's color changed (increase or decrease in brightness), they pressed a button on the button box. A total of 20 fixation point color changes occurred throughout each run; changes to the fixation cross happened at random times with respect to wedge stimulus onsets. We chose to have participants attend fixation, rather than the stimulus position, during the localizer task to reduce contamination of eye movements on any observed decoding effects (Mostert et al., 2018). Generally, systematic eye movement biases are absent or greatly attenuated when participants attend fixation and ignore the peripheral stimulus. With this cross-task training and testing scheme, we would expect that decoding should impaired for all 4 items if participants moved their eyes in the visual search task. Thus, this training-testing scheme protects against the possibility that item-specific target enhancement or distractor suppression effects could be driven by eye movements to a particular item in the display.

Search task. Participants performed a variant of the additional singleton search task (Theeuwes, 1992). On each trial, participants saw a search array containing 4 items (item colors were red, RGB = 255,0,0, or green, RGB = 0,255,0, and presented on a black background, RGB = 0,0,0). The items (2.4º radius) were placed on an imaginary circle 7º from fixation with 1 item in each visual quadrant (i.e., 45º, 135º, 225º & 315º). Participants fixated a small, gray dot (.2º) throughout each run. Participants searched for a "target" (the diamond-shaped item) among distractor items and reported the orientation of the small line inside (line size = .08º x .94º; orientation = horizontal or vertical) by pressing

one of two buttons. Non-singleton distractors, 'non-targets', had the same color as the shape-defined target (e.g., green circles). A "singleton distractor" was present on 66.67% of trials, and was a color singleton (e.g., red circle). Stimuli are illustrated in Figure 1. Note, throughout the manuscript, we will use the word "distractor" to refer to the color-singleton distractors, whereas non-singleton distractors will be referred to simply as "non-targets". Target location (quadrant 1-4), distractor location relative to the target (-90º, +90º, or +180º), distractor presence (66.67% present), and the orientation of the line inside the target (horizontal or vertical) were fully counterbalanced within each run, for a total of 72 trials per run. Search set size was held constant at 4 items. The search array was presented for 2 sec followed by a blank inter-trial interval (equal probability of 2, 3.2, 5, or 8 sec).

We manipulated the degree to which participants were behaviorally captured by the distractor by changing trial history. In "color variable" runs, the colors of targets and distractors swapped unpredictably. In "color constant" runs, the colors of targets and distractors were fixed throughout the run (e.g., the targets and non-singleton distractors were always green and the singleton distractor was always red). Based on prior work (Vatterott and Vecera, 2012; Gaspelin et al., 2017), we expected to observe robust behavioral capture by the singleton distractor in the color variable runs and no behavioral capture in the color constant runs.

Run types were blocked and partially counterbalanced within and across sessions, such that the order of the 2 conditions would be balanced across the 2 sessions for each participant. For example, if in Session 1 a participant first received 4 color variable runs followed by 4 color constant runs (red), then in Session 2 they would first receive 4 color constant runs (green) followed by 4 color variable runs.

Experiment 1b: Behavior

Participants performed the same additional singleton search task described above. Participants viewed the stimuli on CRT monitors (39 x 29.5 cm) from a distance of ~52 cm. Stimulus parameters (size, color) and trial timing were matched to the fMRI experiment. Each experimental block contained a total of 48 search trials. Participants

315 performed a total of 12 blocks of trials (6 color variable, 3 color constant with red targets,
316 3 color constant with green targets). The color constant and color variable conditions were
317 blocked and counterbalanced across participants (half of participants received the color
318 variable condition first).
319
320 **Magnetic resonance imaging acquisition parameters**
321 Scans were performed on a General Electric Discovery MR750 3.0T scanner at
322 the Keck Center for Functional Magnetic Resonance Imaging on the UCSD campus.
323 High-resolution (1mm^3 isotropic) anatomical images were collected as part of the
324 retinotopy session. Most participants' (10 of 12) anatomical images were collected with
325 an Invivo 8-channel head coil; 2 participants' anatomical images were collected with a
326 Nova Medical 32-channel head coil (NMSC075-32-3GE-MR750). GE's "Phased array
327 Uniformity Enhancement" (PURE) method was applied to anatomical data acquired using
328 the 32-channel coil in an attempt to correct inhomogeneities in the signal intensity.
329 Functional echo-planar imaging (EPI) data were collected with the Nova 32 channel coil
330 using the GE multiband EPI sequence, using nine axial slices per band and a multiband
331 factor of eight (total slices = 72; 2 mm^3 isotropic; 0 mm gap; matrix = 104 × 104; field of
332 view = 20.8 cm; repetition time/echo time (TR/ TE) = 800/35 ms, flip angle = 52°; in-plane
333 acceleration = 1). The initial 16 TRs in each run served as reference images for the
334 transformation from *k*-space to image space. Un-aliasing and image reconstruction
335 procedures were performed on local servers and on Amazon Web Service servers using
336 code adapted from the Stanford Center for Cognitive and Neurobiological Imaging (CNI).
337 Forward and reverse phase-encoding directions were used during the acquisition of two
338 short (17 sec) "top-up" datasets. From these images, susceptibility-induced off-resonance
339 fields were estimated (Andersson et al., 2003) and used to correct signal distortion
340 inherent in EPI sequences, using FSL top-up (Smith et al., 2004; Jenkinson et al., 2012).
341
342 **Pre-processing**
343 Pre-processing of imaging data closely followed published lab procedures
344 (Rademaker et al., 2019) using FreeSurfer and FSL. We performed cortical surface gray-

white matter volumetric segmentation of the high-resolution anatomical volume from the retinotopy session using FreeSurfer's "recon-all" procedures (Dale et al., 1999). The first volume of the first functional run from each scanning session was coregistered to this common T1-weighted anatomical image. To align data from all sessions to the same functional space, we created transformation matrices with FreeSurfer's registration tools (Greve and Fischl, 2009), and used these matrices to transform each four-dimensional functional volume using FSL's FLIRT (Jenkinson and Smith, 2001; Jenkinson et al., 2002). After cross-session alignment, motion correction was performed using FSL's McFLIRT (no spatial smoothing, 12 degrees of freedom). Voxelwise signal time-series were normalized via Z-scoring on a run-by-run basis. Analyses after preprocessing were performed using custom scripts in MATLAB 2018A.

fMRI analyses: Inverted encoding model

Voxel selection for Decoding ROIs. We defined visual ROI's using data from the retinotopy session following published lab procedures (Sprague and Serences, 2013; Rademaker et al., 2019). From these retinotopically-derived ROI's, we chose the subset of voxels that were spatially selective for the stimuli used in this task. We thresholded voxels using the independent mapping task data. We ran a one-way ANOVA with factor Quadrant on each voxel; significant voxels ($p < .05$ uncorrected) were retained for analysis. For the aggregate analyses, we *a priori* created an early visual cortex ROI (all spatially selective voxels from V1-V3) and a parietal cortex ROI (all spatially selective voxels from IPS0-3). For individual ROI analyses, we used all individual retinotopic ROIs for which there were a minimum of 90 spatially selective voxels per participant: V1, V2, V3, V3AB, hV4, and IPS0.

Inverted Encoding Model. Following prior work (Brouwer and Heeger, 2009; Sprague and Serences, 2013), we used an inverted encoding model to estimate spatially-selective tuning functions from multivariate, voxel-wise activity within each ROI. We assumed that each voxel's activity reflects the weighted sum of 24 spatially selective channels, each tuned for a different angular location. These information channels are assumed to reflect the activity of underlying neuronal populations tuned to each location.

We modeled the response profile of each spatial channel as a half sinusoid raised to the 24th power:

$$R = \sin(0.5\theta)^{24},$$

where θ is angular location (0–359°, centered on each of the 24 bins from the mapping task), and R is the response of the spatial channel in arbitrary units.

Independent training data B_1 were used to estimate weights that approximate the relative contribution of the 24 spatial channels to the observed response at each voxel. Let B_1 (m voxels × n_1 observations) be the activity at each voxel for each measurement in the training set, C_1 (k channels × n_1 observations) be the predicted response of each spatial channel (determined by the basis functions) for each measurement, and W (m voxels × k channels) be a weight matrix that characterizes a linear mapping from "channel space" to "voxel space". The relationship between B_1, C_1, and W can be described by a general linear model:

$$B_1 = WC_1$$

We obtained the weight matrix through least-squares estimation:

$$\widehat{W} = B_1 {C_1}^{T} \left(C_1 {C_1}^{T}\right)^{-1}$$

In the test stage, we inverted the model to transform the observed test data B_2 (m voxels × n_2 observations) into estimated channel responses, C_2 (k channels × n_2 observations), using the estimated weight matrix, $\widehat{W}$, that we obtained in the training phase:

$$\widehat{C_2} = \left(\widehat{W}^{T}\widehat{W}\right)^{-1}\widehat{W}^{T}B_2$$

Each estimated channel response function was then circularly shifted to a common center by aligning the estimated channel responses to the channel tuned for target location.

Model training and testing. We trained the IEM using independent mapping task data and tested the model using single trial search-task data (average of 4 to 10 TR's after search array onset). We then shifted and averaged the search task data so that like trials were aligned (e.g., rotate and average all trials with target-distractor distance of 90). To reduce idiosyncrasies of only having 1 test set, we iterated the analysis by leaving out 1 block of training data and 1 block of test data, looping through all possible combinations

(e.g., for each 1 block of left out training data, we left out each possible block of test data on different runs of the loop).

Results

Behavior

Subjects performed a variant of the additional singleton search task (Theeuwes, 1992) (Figure 1A) in which they searched for a target (diamond) among non-targets (circles). On each trial, the participant reported via button-press the orientation of the line inside the diamond target (vertical or horizontal). On 66.67% of trials, one of the non-targets was uniquely colored ("singleton distractor present", e.g., one red distractor, two green non-targets, and one green target item). Behavioral capture was quantified as slowed response times (RTs) when the distractor was present versus absent. In addition to examining the basic capture effect, a key goal of this work was to examine modulation of capture by trial history (Vatterott and Vecera, 2012; Gaspelin et al., 2015, 2017). Prior work has shown that participants can learn to suppress a distractor (i.e., no RT difference for singleton distractor present versus absent trials) when the same distractor color or distractor location is repeated over many trials (Vatterott and Vecera, 2012; Gaspelin et al., 2015, 2017). Building on this work, we included two key task conditions in a counterbalanced, block-wise fashion to manipulate trial history and behavioral capture while using identical stimulus arrays (e.g., green target, red distractor). In the color constant condition (Figure 1A), the array colors stayed constant throughout the block (e.g., green target, green non-target items, red distractor). In the color variable condition (Figure 1B), the array colors randomly varied from trial to trial. Based on prior work, we expected robust capture in the color variable condition, and little or no capture in the color constant condition (Vatterott and Vecera, 2012; Gaspelin et al., 2015, 2017).

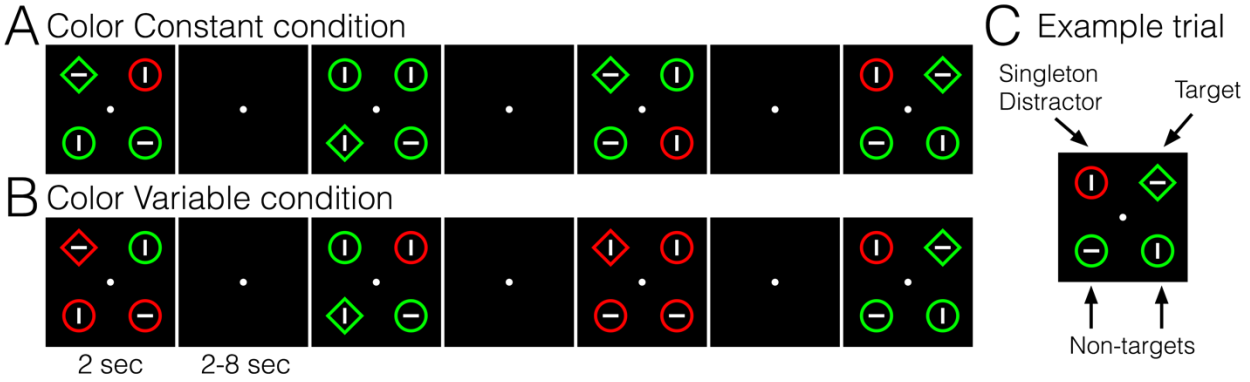

Figure 1. Visual search task stimuli. On each trial, participants viewed a 4-item array and reported the orientation of the line inside the diamond-shaped target (horizontal or vertical). **(A)** In the color constant condition, colors of targets and singleton distractors were fixed throughout the run. **(B)** In the color variable condition, colors of targets and singleton distractors swapped randomly from trial to trial. **(C)** An example trial with labels for the target, singleton distractor, and non-target items.

Replicating prior work, we found significant behavioral capture that was modulated by trial history (Geyer et al., 2006; Vatterott and Vecera, 2012; Goschy et al., 2014; Gaspelin et al., 2015, 2017; Wang and Theeuwes, 2018a; Failing et al., 2019a). In our MRI sample (Exp 1a, Figure 2A & 2C), we observed significant behavioral capture in the color variable condition, with longer RT's for distractor present versus distractor absent trials (M = 32.8 ms, SD = 25.5 ms, p = .001, d = 1.28), but capture was not significant in the color constant condition (M = 10.8 ms, SD = 18.5 ms, p = .07, d = .59). Importantly, capture was significantly larger for color variable vs. color constant runs (p = .009, d = .91). We replicated this pattern of findings in the behavior-only experiment (Exp. 1b, Figure 2B & 2D), with robust capture for 'color variable' ($p < 1 \times 10^{-5}$, d = 1.31), no significant capture for 'color constant' (p = .1, d = .32), and larger capture for color variable vs. constant (p = .002, d = .71). Participants in both experiments were accurate overall (>90%), and there was no evidence of a speed-accuracy trade-off (Figure 2-1).

In addition to the key modulation of capture as a function of stimulus history, we also replicated prior findings that the degree of capture is significantly modulated by the physical distance between the target and the distractor (Mounts, 2000; Turatto and Galfano, 2001; Wang and Theeuwes, 2018a; Failing et al., 2019b), with larger capture for distractors nearer the target (Figure 2E-F). We ran a repeated measures ANOVA

including both experiments (n=36). Including Experiment as a factor revealed no experiment main effects or interactions ($p > .2$), so the two experiments were combined for further analyses of the behavioral data (although Figure 2 shows data from the two experiments separately). There was a significant effect of Condition (larger capture for color variable than color constant), $p < 1x10^{-4}$, a main effect of Distance (larger capture for 90° than 180°), $p = .037$, $\eta^2_p = .12$, and an interaction between Condition and Distance (greater distance effect in the color variable condition), $p = .014$, $\eta^2_p = .16$.

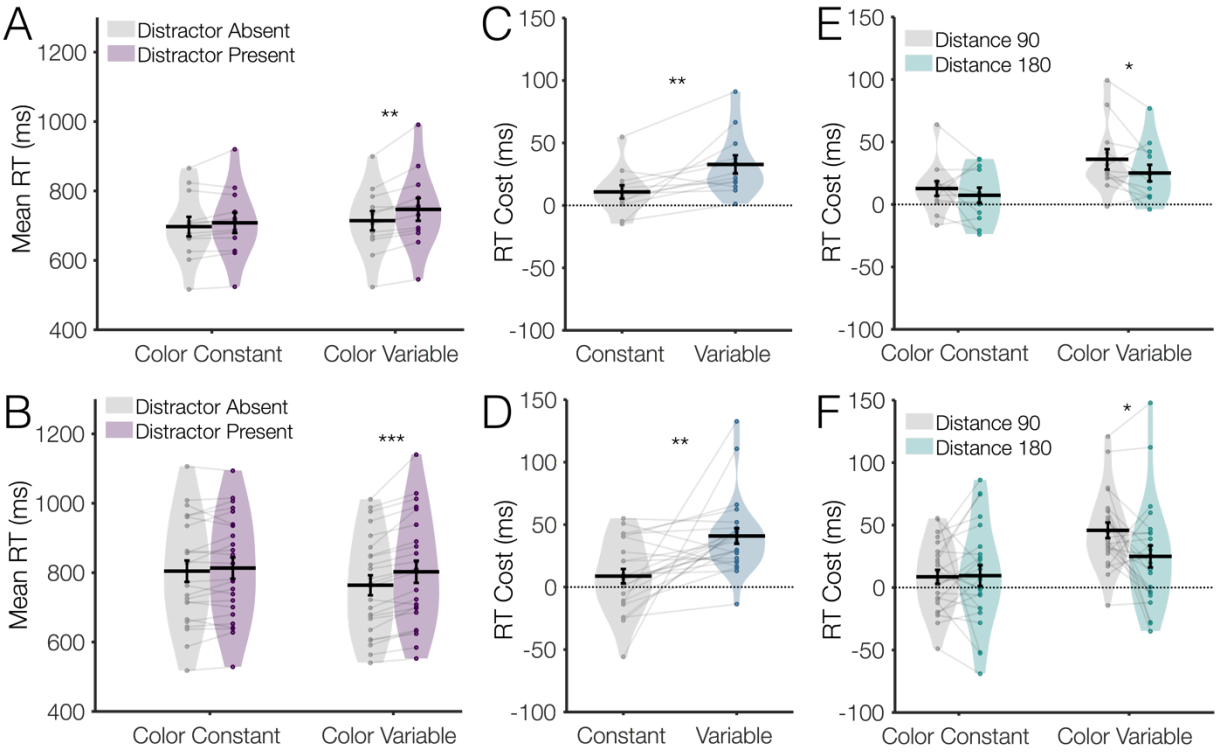

Figure 2. Behavioral capture during the visual search task. (A) In the main MRI Experiment (Exp 1a), participants were significantly captured by the salient singleton distractor in the color variable condition, but not in the color constant condition. **(B)** This pattern replicated in the behavior-only experiment (Exp 1b). **(C-D)** Capture costs (RT Difference for distractor present – absent trials) were significantly larger in the color variable than in the color constant condition in Exp 1a **(C)** and Exp 1b **(D)**. **(E-F)** Capture costs (RT Difference for distractor present – absent trials) were significantly modulated by the distance between the target and distractor in the color variable condition both in Exp 1a **(E)** and Exp 1b **(F)**. Violin plot shading shows range and distribution of the data; dots represent single subjects; black error bars indicate ±1 SEM. Asterisks depict significance for uncorrected post-hoc comparisons between adjacent bars within each experiment, * $p < .05$, ** $p < .01$, *** $p < .001$.

fMRI results: Model estimates of spatial position in the independent mapping task

We opted for a multivariate model-based approach to estimate the amount of information encoded in voxel activation patterns about each of the 4 stimuli in the search array, as such multivariate approaches are more sensitive than just computing the univariate mean response across all voxels (Cox and Savoy, 2003; Haynes and Rees, 2005; Kamitani and Tong, 2005; Norman et al., 2006; Serences and Saproo, 2012; Tong and Pratte, 2012). For example, item-specific information has been observed using multivariate methods even in the absence of univariate changes (Lewis-Peacock and Postle, 2012; Emrich et al., 2013) (but for univariate analyses of the present data, see extended data Figure 3-1). We opted for an inverted encoding model (IEM) approach (Sprague et al., 2018a, 2019), as opposed to Bayesian or other decoders (van Bergen et al., 2015; van Bergen and Jehee, 2019), because this approach allowed us to easily derive a separate estimate of the information encoded about each of the 4 simultaneously presented items from the search array in the main analysis (Sprague et al., 2019). For further discussion of IEM model assumptions and best practices, see: (Sprague et al., 2018a, 2019).

In our key analyses of the fMRI data, we used an independent mapping task to train a model of spatial position from which we estimated the relative priority of all item positions within the visual search array. During the independent mapping task, observers viewed a flickering checkerboard wedge that was presented at 1 of 24 positions on an imaginary circle around fixation (Figure 3A). We first checked that we observed robust estimates of spatial position when training and testing within the independent mapping task (leave 1 run out, see section 'Inverted Encoding Model'). We observed robust model-based estimates of spatial position for all ROIs (Figure 3B). Parameters from the best-fitting von Mises distribution to each region-of-interest (ROI) are depicted in Figure 3C (model fits, linear classifier results, and von Mises parameters for shuffled data are shown in extended data Figure 3-2). There was an effect of ROI on precision such that spatial position was represented less precisely in later visual areas ($p < 1\text{x}10^{-5}$, where precision is the concentration parameter κ of the best fitting von Mises, with higher values indicating a more precise function). There was also an effect of ROI on the amplitude and baseline

measures of the model-based estimates of spatial position ($p < 1x10^{-5}$), and all 3 parameters significantly differed from zero across all ROIs ($p < 1x10^{-5}$). These results, particularly the observation of amplitudes greater than 0, confirmed that activation patterns in all examined regions encode information about spatial position.

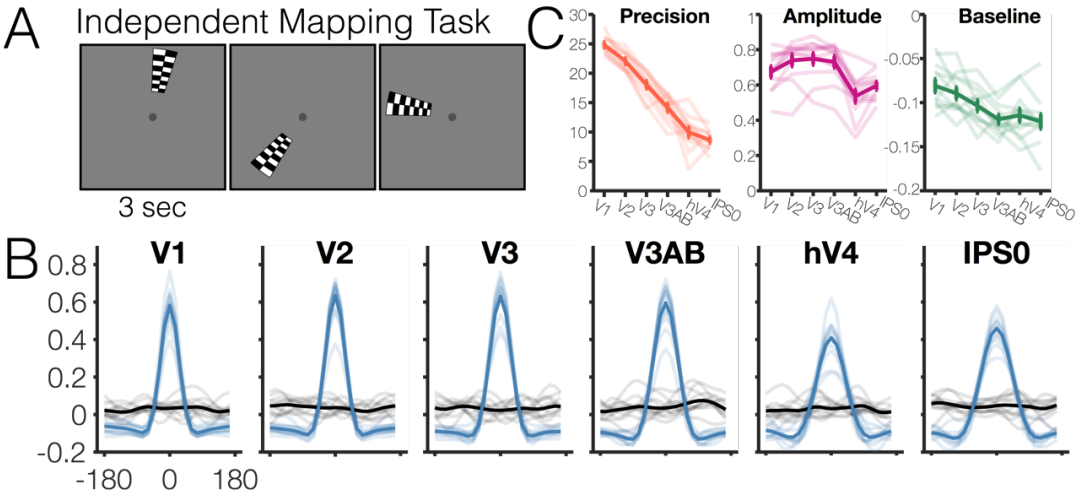

Figure 3. Single-item model estimates training and testing within the independent mapping task. (A) Independent mapping task used to train the model to estimate spatial position of 4 search array items. Participants viewed a flickering checkerboard which could appear at one of 24 positions around an imaginary circle. **(B)** Blue lines: Model estimates of viewed spatial position training and testing within the independent mapping task. Single-trial model estimates for each subject are aligned to 0 degrees and averaged. Black lines: Model estimates for shuffled training labels. Opaque lines = group average; semi-transparent lines = individual subjects. **(C)** Descriptive statistics for best fit von Mises parameters (precision [κ], amplitude, baseline) to model estimates in panel B. Error bars indicate ±1 SEM; the opaque line shows the group average; semi-transparent lines show individual subjects.

Unlike the single item model estimates that were derived based on the independent mapping task (Figure 3), we could not fit a simple, uni-modal Gaussian function to model-based estimates derived from the search task data because 4 peaks in the model output were expected – one for each item in the search array. As such, we first conducted simulations to ensure that we would be able to measure putative changes to individual item representations (e.g. target enhancement, distractor suppression), despite multiple item representations contributing to the aggregate 4-item model estimates. To

do so, we used data from the independent mapping task to generate predictions for observed model responses in a 4-item array. For each ROI, we took the 1-item model response derived from the independent mapping task, replicated this model response four times (once at each of the four search array positions), and took the average of all 4 shifted 1-item model response lines to generate a single 4-item model prediction. In addition, we systematically varied the strength of the simulated response to each item to ensure that we were able to recover a corresponding change in the item-specific responses estimated from the aggregate 4-item model estimate (Figure 4; extended data Figure 4-1).

These simulations revealed clearly separable peaks for all four items in early areas like V1, where spatial precision is high (Figure 4A-B, left panel). In contrast, identifying clear peaks in later areas like IPS0 was difficult when the response to all items was equivalent (Figure 4A-B, right panel). However, if one item evoked a larger or smaller response than the other items, as would be expected with target enhancement or distractor suppression, then clear and measurable changes to the aggregate 4-item model estimates emerged (Figure 4C). Further simulations showed that we could detect smaller changes to one item (e.g., distractor suppression) in the presence of larger changes to another item (e.g., target) by measuring the response amplitude at each expected item's peak. In V1, this is clearly seen in the peak response to each item; in later areas such as IPS0, such changes manifest as a large central peak that is skewed by the neighboring items' smaller changes (Figure 4D).

We also used a general linear model (GLM) to estimate best-fitting gain factors for each of the 4 hypothesized item representations by fitting an aggregate function and allowing one parameter in the GLM to scale the response associated with each item. This is essentially the inverse of the simulations described above: For a given aggregate response (i.e., the response of each of the 24 spatial channels when shown a given 4-item search array), we used a non-negative least squares solution(Lawson and Hanson, 1974) to estimate the contribution of each of the 4 item positions (calculated from the 1-item localizer task) to the observed 4-item search array response (Figure 4E). This analysis yielded similar results to the simple approach of comparing the height at each

565 expected item peak (extended data Figure 5-4). Thus, using either the raw amplitude at
566 expected peaks or a GLM-based approach, we determined that we should be able to
567 accurately characterize situations in which there was no modulation of target and
568 distractor responses as well as situations in which there was a significant modulation of
569 target and/or distractor responses.
570

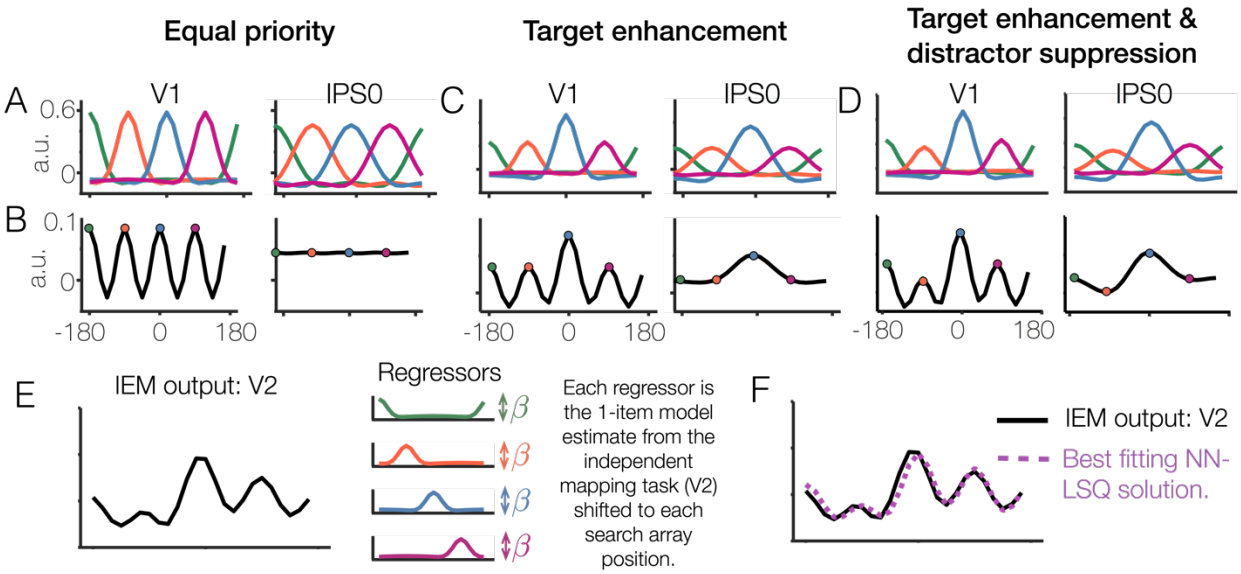

571

572 **Figure 4. Generating predictions for 4-item model estimates by averaging single-**
573 **item model estimates from the independent mapping task. (A)** Average from the
574 independent mapping task plotted at 4 hypothetical item locations. Here, these 4 "items"
575 are represented with equal priority. (B) Hypothetical observed response when measuring
576 a single trial containing the 4 items presented simultaneously. This line is the average of
577 all lines in Panel A. (C) The same as panels A and B, but with the item at position 0
578 assigned a higher response amplitude than the other three items. (D) The same panels
579 as A and B, but with both an enhanced item at position 0 and a suppressed item at position
580 -90. (E) Actual IEM model output for 4-item search arrays in V2 (Target plotted at 0,
581 distractor plotted at -90). To estimate the strength of each of the 4 underlying item
582 representations, one can simply measure the height (a.u.) at expected item peaks (i.e., -
583 180, -90, 0, and 90). Alternatively, one may use a non-negative least squares solution to
584 estimate weights for a regressor for each of the 4 item positions. Each regressor is the 1-
585 item IEM output from the independent mapping task within the same region (e.g., V2),
586 shifted to the appropriate item location. (F) Example IEM output and best-fitting non-
587 negative least squares solution with 4 item regressors.
588

589

590

Analysis of search array locations in V1, V2, V3, V3AB, hV4, and IPS0.

Given that we can assess differential responses associated with each of the 4 items in the search array (Figure 4), we next tested whether goal- and history-driven modulations were differentially represented across the visual stream by performing an analysis of history-driven effects on target and distractor processing across visual ROIs (Figure 5). These six ROIs (V1, V2, V3, V3AB, hV4 and IPS0) were chosen for each participant having at least 90 spatially selective voxels as determined by the localizer data. Here, we focus on history-driven effects on target processing and distractor processing for the arrays where behavioral and neural distractor competition effects were greatest (target-distractor separation +/-90°, see Figure 2E,F). Full ANOVA results and additional plots are shown for individuals ROIs with both array 90° and 180° configurations in extended data Figures 5-4 and 5-5.

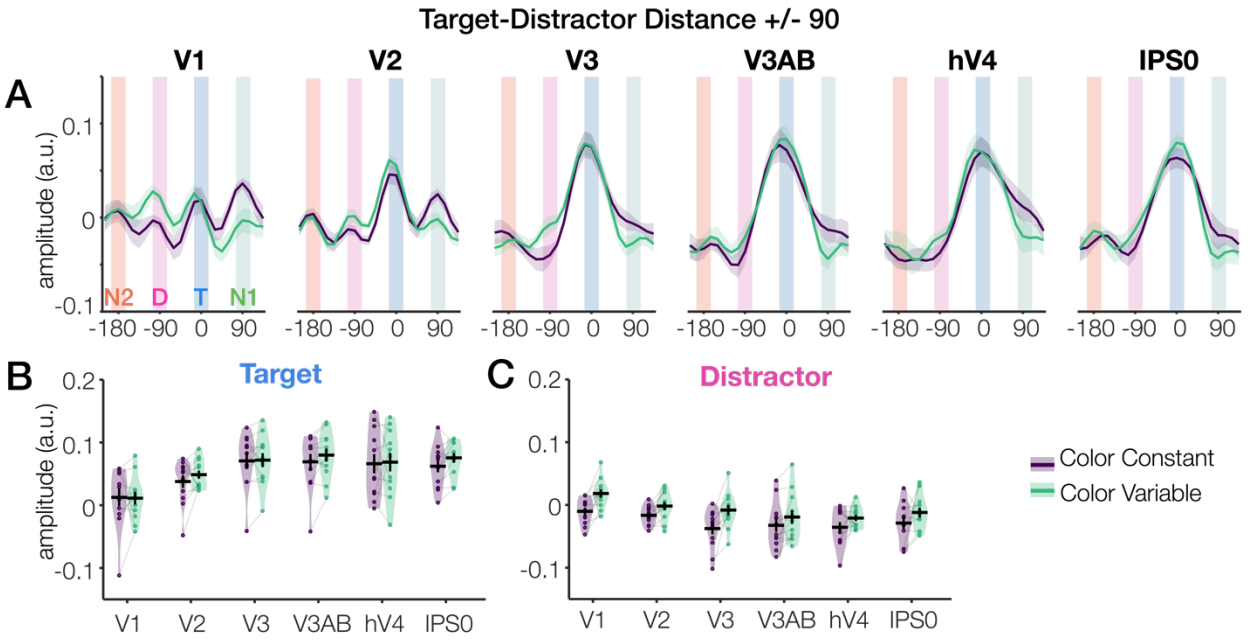

Figure 5. Dissociable effects of stimulus history on target enhancement and distractor suppression. (A) Model responses for individual ROIs as a function of task condition (Arrays with target-distractor distance +/-90). Purple and green lines (Shaded error bars = 1 SEM) show the output of the inverted encoding model in the color constant and color variable conditions, respectively. Background panels at -180°, -90°, 0° and +90° show the positions of the 4 search array items (blue = target (T), pink = distractor (D), green = non-target 1(N1), orange = non-target 2 (N2). Target enhancement can be seen as the greater height at position 0: The IEM peak at the blue bar is higher than the IEM peak at the orange, pink, and green bars. History-driven distractor suppression can be seen as the lower height at position -90 for the color constant vs. color variable conditions: The IEM peak at the pink bar is higher for the green line than for the purple line. (B) Target amplitude as a function of ROI and task condition. There was no effect of task condition on target amplitude, but a significant increase in target amplitude across ROIs. Violin plot shading shows range and distribution of the data; dots represent single subjects; black error bars indicate ±1 SEM. (C) Distractor amplitude as a function of ROI and task condition. There was a significant effect of task condition on distractor amplitude, and this history-driven effect did not interact with ROI.

We found evidence for within-display target enhancement (i.e., enhancement of the target over other positions), but we did not find evidence for history-driven modulations of target enhancement. Overall target enhancement was significant in all ROIs (all *p*'s < .001) except for V1 (*p*'s > .12), and target enhancement significantly increased across ROIs ($p < .001$) as shown in Figure 5A-B. There was, however, no meaningful effect of history on target amplitude as revealed by a repeated-measures

ANOVA testing the main effect of history and the interaction between history and ROI on target processing (p = .35, η^2_p = .08; p = .64, η^2_p = .04 for main effect and interaction respectively). This pattern was the same whether we used raw amplitude values or we used values from the GLM (no effect of history, p = .28, no interaction of history and ROI, p = .51).

In contrast, history had a significant effect on distractor amplitude such that distractor amplitudes were significantly attenuated in the color constant condition relative to the color variable condition. A repeated-measures ANOVA revealed a main effect of history (p = .007, η^2_p = .50) and no interaction between history and ROI (p = .44, η^2_p = .08), indicating that the effect of history on distractor processing was similar throughout the examined ROIs. Though the ANOVA suggests that history effects were of a similar magnitude across all examined ROIs, a post-hoc simple main effects analysis showed that the effect was individually significant only in V1 ($p < .001$) and V3 ($p < .01$). This general pattern was the same whether we used raw amplitude values or else used values from the GLM approach (main effect of history, p = .01, η^2_p = .47, no interaction of history and ROI, p = .87, η^2_p = .03).

Finally, we examined changes in non-target responses. For “non-target 1” (the item neighboring the target on the side opposite the distractor), there was an overall history related modulation (color constant > color variable, p = .016, η^2_p = .42) that did not interact with ROI (p = .76, η^2_p = .03). Similar general effects on non-target processing have been observed recently (Won et al., 2020) and may reflect a bias of attention away from the distractor such that attention may ‘overshoot’ the target because of the reduction in signal at the distractor location. The effect of history on “non-target 1” responses likewise was similar though of borderline significance in the GLM analysis (color constant > color variable, p = .049, η^2_p = .31). We found no effect of history on the other non-target (“non-target 2”) which occupied the spatial position 180 degrees from the target item ($p >= .61$).

Finally, additional analyses on larger, aggregate ROIs (V1-V3, IPS0-3) yield convergent results and also demonstrate how distractor suppression effects were absent for arrays where the target and distractor did not compete with each other (target-distractor separation +/- 180°), consistent with our separate analysis of each ROI (Figure

676 6) and prior behavioral and neural findings (Turatto and Galfano, 2001; Wang and
677 Theeuwes, 2018a; Failing et al., 2019b; Won et al., 2020) (extended data Figures 5-1, 5-
678 2, and 5-3).
679
680 **Discussion**
681 To find what we are looking for, we must integrate information about stimulus
682 relevance, salience, and history. While the impact of stimulus relevance and salience on
683 topographically organized population codes have been thoroughly investigated, stimulus
684 history is not thought to be a wholly goal-driven or stimulus-driven process. Rather, history
685 effects may depend on interactions between the current stimulus drive ('bottom-up' factor)
686 and the current internal state of the visual system ('top-down' factor). To address this
687 ambiguity and to better understand how history impacts visual processing, we tested
688 whether history-driven changes to attentional priority operate in a manner akin to
689 canonically goal-driven and/or to stimulus-driven signatures of priority. To do so, we
690 estimated population-level neural responses evoked by 4-item search arrays across
691 retinotopically-defined areas of occipital and parietal cortex. We found that stimulus
692 history did not modulate the specificity of goal-driven target templates, as goal-driven
693 target enhancement was unaffected by stimulus history. Instead, we found that stimulus
694 history attenuated responses related to distractors throughout the visual hierarchy. These
695 results suggest that stimulus history may influence visual search performance via local
696 competitive interactions within early sensory cortex (i.e., V1), consistent with the V1
697 salience map hypothesis. Further, we argue that these early competitive interactions
698 cannot be explained by goal-driven predictive coding models.
699
700 **Proposed model: Adaptation alters a stimulus-driven salience map in V1**
701 Models of image-computable salience propose that local image statistics
702 determine competitive interactions that give rise to 2D spatial salience maps within V1
703 (Li, 2002; Zhang et al., 2012) or after integrating feature maps at a later stage of
704 processing (e.g., Treisman and Gelade, 1980; Wolfe, 1994; Itti and Koch, 2000; Carmi
705 and Itti, 2006), and these models do not typically account for the long-term effects of

stimulus history. Note, many existing saliency models do account for *short -term* changes to stimuli by coding for dynamic image factors such as motion velocity and flicker (i.e., luminance onset or offset) across movie frames (~30 ms per frame), (Itti and Koch, 2000; Carmi and Itti, 2006). However, these dynamic feature maps cannot explain history effects that build up over the course of many trials and persist across blank inter-trial intervals. Rather, an additional mechanism is needed to integrate stimulus information over a longer duration. Recent work suggests that neural adaptation – which is linked to the history of prior stimuli – in a subset of tuned neurons may alter stimulus-driven competitive dynamics (e.g., divisive normalization, Carandini and Heeger, 2012) within early visual cortex (Solomon and Kohn, 2014). Thus, to accommodate our observation of history-driven distractor suppression within existing saliency models, we propose that stimulus-driven evoked responses in V1 may be integrated over a longer, multi-trial duration (as opposed to just within a single image; Figure 6) (Karni and Sagi, 1991; Schwartz et al., 2002; Jehee et al., 2012). In the context of models of visual search, this might be comprised of a series of 2D spatial maps that together form a temporally integrated 3D salience map (i.e., salience is computed based on current and prior physical stimulus properties). Consistent with the notion of a 3D salience map, recent behavioral and neural evidence suggests a role for priming and habituation in visual search behaviors (Geyer et al., 2006; Feldmann-Wüstefeld and Schubö, 2016; Turatto and Pascucci, 2016; Turatto et al., 2018; Won and Geng, 2020, also see: Reavis et al., 2016), even when the adapting stimuli are task-irrelevant.

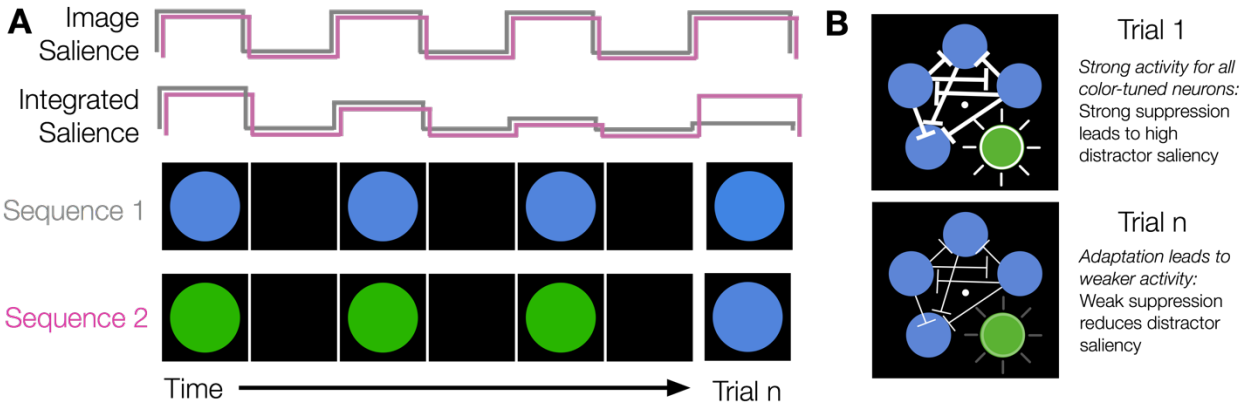

Figure 6. Simplified cartoon illustration of local-image versus temporal-integration salience for a simple image with one feature and location. (A) In 2-D salience computations, stimulus-driven stimulus drive is determined locally within a given image without respect to prior images. Sequence 1 is 4 different trials, and on each trial the same stimulus is shown (Blue-Blue-Blue-Blue). Sequence 2 is 4 different trials, but the final trial is a different color from the preceding trials (Green-Green-Green-Blue). The final trial (Blue) is physically identical for the two sequences. So, the final stimuli (trial n in each sequence) have identical 2-D salience. Assuming that we chose equiluminant green and blue values, then each "frame" in the sequence likewise has approximately the same image-computable salience, as shown by the uniform-sized square pulses in the cartoon. Alternatively, stimulus-driven salience maps may better be conceived of as reflecting a temporally-integrated 3-D salience map, as early sensory neurons adapt to ongoing stimulus features. In Sequence 1 (Blue-Blue-Blue-Blue), the activity of neurons that are maximally responsive to blue wanes due to adaptation. In Sequence 2 the activity of neurons maximally responsive to green wanes over the first 3 trials, but the final stimulus elicits a robust response from the non-adapted blue-preferring neurons. Thus, temporally-integrated salience for the trial *n* in each sequence differs across the two sequences even though the stimuli are physically identical. (B) Most studies of predictive coding and adaptation consider changes to neural activity for a single item. Here, we illustrate how adaptation can have consequences for stimulus-driven saliency that arises from inter-item competition within multi-item arrays (e.g., Itti and Koch, 2000). Top: For the first presentation of the array, all neurons respond strongly, leading to classic inter-item competition effects that yield high distractor saliency. Bottom: With repeated presentations and adaptation, overall activity and inter-item competition is weakened, yielding a relative attenuation of the distractor.

Consistent with a temporally-integrated V1 saliency account of history-driven distractor suppression, we observed history-driven modulations only with sufficient competition (i.e., targets and distractors were closer together) and we observed robust history-driven modulations in V1 in the absence of goal-driven modulations. In line with our findings, prior behavioral work has shown that incidental repetitions of distractor, but

not target, features and locations modulate search performance (Geyer et al., 2006; Failing et al., 2019b). Likewise, prior work has shown a rapid suppression of distractor-evoked neural responses (Hickey et al., 2009; Zhang and Luck, 2009; Sawaki and Luck, 2010; Gaspar and McDonald, 2014; Moher et al., 2014; Gaspelin et al., 2015, 2017) and that the likelihood of distraction results in anticipatory changes to distractor, but not target, locations (Serences et al., 2004; Heuer and Schubö, 2019; Won et al., 2020). However, the proposed temporally-integrated salience account does not capture all history-driven effects. In our task, the repeated distractor features were purely visual in nature, and thus history effects might be mediated entirely via local circuit dynamics (i.e., the adaptation account described above). In contrast, other studies have examined history-driven effects for more abstract features like reward (Mazer and Gallant, 2003; Serences, 2008; Saproo and Serences, 2010; Stanisor et al., 2013; Chelazzi et al., 2014; Hickey and Peelen, 2015; MacLean and Giesbrecht, 2015; Itthipuripat et al., 2019; Kim and Anderson, 2019) (but also see: Maunsell, 2004; Anderson and Kim, 2019), which may require an intermediary pathway such as the medial-temporal lobe (Theeuwes, 2019) or dopaminergic midbrain structures (Hickey and Peelen, 2015, 2017).

Implications for predictive coding theories of visual processing

Much of the debate about history-driven changes to visual search has been separated from the predictive coding literature, but these two ideas are highly intertwined. Predictive coding theories propose that incoming visual information is compared to expected visual information at later stages of processing (Rao and Ballard, 1999; Friston, 2005; Summerfield and de Lange, 2014; Spratling, 2017). Efficient, predictive coding is achieved via an iterative updating process whereby error units detect deviations from what is expected and inhibit expected information in the prediction units at an earlier stage of processing. Here, we consider whether an expectation-driven predictive coding account, whereby top-down expectations about the upcoming stimulus influence neural processing, could likewise explain the pattern of results that we have observed. We note that the term “predictive coding” has been used in a wide variety of ways in the literature (Spratling, 2017), some of which are entirely stimulus-driven (e.g., within the retina;

Srinivasan et al., 1982). Here, we are concerned with considering versions of predictive coding whereby top-down expectations influence stimulus processing.

A fundamental tension has long been noted in the literature: Predictive coding models primarily explain how expected information becomes *attenuated,* and thus have difficulty explaining signal enhancement related to attention (e.g., Luck et al., 1997; Hupé et al., 1998; Kastner and Ungerleider, 2000). Many predictive coding models implement error-driven feedback as inhibitory signaling from the next adjacent visual area (e.g., V3 to V2). To explain top-down attentional prioritization effects, predictive coding models must be modified, as has been done in the Predictive Coding/ Biased Competition (PC/BC) model (Spratling, 2008). In this model, an additional top-down attention component is added, and the error and prediction units are shifted such that error-driven feedback is excitatory. These changes to the model allow for biased competition effects to arise within a predictive coding framework.

Although the PC/BC model variants can predict biased competition effects in attention, such models critically predict that target enhancement and distractor suppression effects will be yoked, as both effects arise from feedback from the next higher level of visual processing. Thus, for existing predictive coding models to explain our results, we should have observed that the emergence of history-driven distractor suppression paralleled top-down target enhancement. In contrast, we found diverging target enhancement and history-driven distractor suppression effects: whereas target enhancement was absent in V1 and increased across the visual stream, history-driven distractor suppression emerged in V1. Thus, we propose that history-driven distractor suppression is best explained by 'bottom-up' inter-trial priming arising from adaptation within V1 (Westerberg et al., 2019).

Furthermore, we argue that it is important to differentiate between "bottom-up" and "top-down" expectational effects, analogous to recent arguments that it is critical to differentiate between potential confounds of attention and expectation (Summerfield and de Lange, 2014; Rungratsameetaweemana and Serences, 2019). We define 'top-down' expectations as those that can be updated flexibly and on a rapid time scale (e.g., over the course of a few trials). In contrast, we define 'bottom-up' expectations as those that

are ingrained over a very long time-scale and tied to particular stimuli. For example, early ideas about predictive coding emerged from studies of the retina: By exploiting long-term 'expectations' that naturalistic stimuli are correlated in space and time, coding within the retina can be highly efficient (Srinivasan et al., 1982; Rao and Ballard, 1999).

Making a distinction between 'bottom-up' and top-down' expectations can explain prior results that run counter to some predictive coding models. Specifically, Maljkovic and Nakayama's (1994) priming of pop-out experiments demonstrated that RT costs are incurred by switching stimuli even when the stimulus switch is expected. When a stimulus is predictable and repeated (e.g., 0% probability of a color switch), participants are faster than when a stimulus is unpredictable and switches color (e.g., 50% probability of a color switch. If expectations can attenuate the cost of switching colors, then participants should likewise be faster in a predictable, 100% switch condition than in the unpredictable 50% switch condition. In contrast to this prediction, Maljkovic & Nakayama found that participants were *slower* in the 100% switch condition: Participants apparently were unable to use their expectations to overcome bottom-up stimulus-driven priming effects.

Goal-driven attention effects

In addition to implicating early visual cortex in representing history-driven task factors during visual search, we also replicated prior findings that the locations of attended items (here, search targets) are prioritized relative to other item locations in both visual and parietal cortex (Saproo and Serences, 2010; Sprague and Serences, 2013; Sprague et al., 2018b). These target-related modulations are consistent with the broad involvement of visually-responsive regions in representing goal-driven priority during visual search (Mazer and Gallant, 2003; Ogawa and Komatsu, 2006). For example, recent studies manipulated the salience (contrast) and relevance (attended or unattended) of items and found that salience and relevance were both represented, to varying degrees, across the visual hierarchy (Poltoratski et al., 2017; Sprague et al., 2018b). Notably, however, here we found that target prioritization was absent in V1, whereas prior work has found robust effects of attention in V1 (Motter, 1993; Kastner, 1998; Tootell et al., 1998; Gandhi et al., 1999; Kastner et al., 1999; Somers et al., 1999; Serences and Yantis, 2007; Saproo and

Serences, 2010; Sprague and Serences, 2013). This difference may reflect task differences — much prior work found attention-related gains in V1 when spatial attention was cued in advance or a single target was shown, whereas visual search arrays provide visual drive at many competing locations and spatial attention is deployed only after array onset. As such, further work may be needed to unconfound history effects and attention effects in the study of spatial attention, as much early work on univariate attention effects has employed blocked designs where the same location is attended for many trials in a row (Kastner, 1998; Tootell et al., 1998; Gandhi et al., 1999; Kastner et al., 1999; Somers et al., 1999).

Future directions

Although our work suggests that stimulus history modulates representations of distractor but not target processing in visual cortex, there are some potential limitations to the current design that suggest avenues for future work. First, because we measured only location, we could not directly measure suppression of the distractor color (Failing et al., 2019a). However, as the spatial position of the distractor was completely unpredictable, our results do strongly imply that the distractor color was suppressed. Likewise, most theories of visual search hypothesize that space is the critical binding medium through which feature and goal maps are integrated (Treisman and Gelade, 1980; Wolfe, 1994; Itti and Koch, 2000), and recent work suggests that location is spontaneously encoded even when only non-spatial features such as color are task-relevant (Foster et al., 2017a). Second, it is possible that history may modulate both distractor- and target-processing in other circumstances not tested here. That is, perhaps the target template ‘diamond’ in our task was sufficiently useful such that adding feature information to this template (e.g., ‘red diamond’ rather than ‘diamond’) did not confer a behavioral advantage (but see: Maljkovic and Nakayama, 1994). Finally, the time-course of MRI (sampling every 800 ms) is slower than shifts of spatial attention to the search target (< 500 ms) (Foster et al., 2017b). Although the history-driven effects that we observed in visual cortex are consistent with the rapid distractor suppression effects observed in EEG (Sawaki and Luck, 2010; Gaspar and McDonald, 2014), we cannot

definitively say on the basis of these data that the observed history-driven effects occurred rapidly and directly within visual cortex versus via recurrent feedback from later visual areas. Nonetheless, the present work is consistent with and provides critical initial evidence for such a model.

References

Anderson BA, Kim H (2019) On the relationship between value-driven and stimulus-driven attentional capture. Atten Percept Psychophys 81:607–613.

Andersson JLR, Skare S, Ashburner J (2003) How to correct susceptibility distortions in spin-echo echo-planar images: application to diffusion tensor imaging. NeuroImage 20:870–888.

Arita JT, Carlisle NB, Woodman GF (2012) Templates for rejection: Configuring attention to ignore task-irrelevant features. Journal of Experimental Psychology: Human Perception and Performance 38:580–584.

Awh E, Belopolsky AV, Theeuwes J (2012) Top-down versus bottom-up attentional control: a failed theoretical dichotomy. Trends in Cognitive Sciences 16:437–443.

Beck VM, Hollingworth A (2015) Evidence for negative feature guidance in visual search is explained by spatial recoding. Journal of Experimental Psychology: Human Perception and Performance 41:1190–1196.

Beck VM, Hollingworth A, Luck SJ (2012) Simultaneous Control of Attention by Multiple Working Memory Representations. Psychol Sci 23:887–898.

Becker MW, Hemsteger S, Peltier C (2015) No templates for rejection: a failure to configure attention to ignore task-irrelevant features. Visual Cognition 23:1150–1167.

Bisley JW, Mirpour K (2019) The neural instantiation of a priority map. Current Opinion in Psychology 29:108–112.

Bogler C, Bode S, Haynes J-D (2011) Decoding Successive Computational Stages of Saliency Processing. Current Biology 21:1667–1671.

Brainard DH (1997) The Psychophysics Toolbox. Spat Vis 10:433–436.

Brouwer GJ, Heeger DJ (2009) Decoding and Reconstructing Color from Responses in Human Visual Cortex. Journal of Neuroscience 29:13992–14003.

Carandini M, Heeger DJ (2012) Normalization as a canonical neural computation. Nat Rev Neurosci 13:51–62.

Carlisle NB, Arita JT, Pardo D, Woodman GF (2011) Attentional Templates in Visual Working Memory. Journal of Neuroscience 31:9315–9322.

Carmi R, Itti L (2006) Visual causes versus correlates of attentional selection in dynamic scenes. Vision Research 46:4333–4345.

915 Chelazzi L, Eštočinová J, Calletti R, Lo Gerfo E, Sani I, Della Libera C (2014) Altering Spatial Priority
916 Maps via Reward-Based Learning. Journal of Neuroscience 34:8594–8604.

917 Conci M, Deichsel C, Müller HJ, Töllner T (2019) Feature guidance by negative attentional templates
918 depends on search difficulty. Visual Cognition 27:317–326.

919 Cox DD, Savoy RL (2003) Functional magnetic resonance imaging (fMRI) "brain reading": detecting and
920 classifying distributed patterns of fMRI activity in human visual cortex. NeuroImage 19:261–270.

921 Dale AM, Fischl B, Sereno MI (1999) Cortical Surface-Based Analysis. NeuroImage 9:179–194.

922 Desimone R, Duncan J (1995) Neural Mechanisms of Selective Visual Attention. Annu Rev Neurosci
923 18:193–222.

924 Downing PE (2000) Interactions Between Visual Working Memory and Selective Attention. Psychol Sci
925 11:467–473.

926 Emrich SM, Riggall AC, LaRocque JJ, Postle BR (2013) Distributed Patterns of Activity in Sensory Cortex
927 Reflect the Precision of Multiple Items Maintained in Visual Short-Term Memory. Journal of
928 Neuroscience 33:6516–6523.

929 Engel SA, Furmanski CS (2001) Selective Adaptation to Color Contrast in Human Primary Visual Cortex.
930 J Neurosci 21:3949–3954.

931 Engel SA, Rumelhart DE, Wandell BA, Lee AT, Glover GH, Chichilnisky E-J, Shadlen MN (1994) fMRI of
932 human visual cortex. Nature 369:525–525.

933 Failing M, Feldmann-Wüstefeld T, Wang B, Olivers C, Theeuwes J (2019a) Statistical regularities induce
934 spatial as well as feature-specific suppression. Journal of Experimental Psychology: Human
935 Perception and Performance 45:1291–1303.

936 Failing M, Wang B, Theeuwes J (2019b) Spatial suppression due to statistical regularities is driven by
937 distractor suppression not by target activation. Atten Percept Psychophys 81:1405–1414.

938 Fecteau J, Munoz D (2006) Salience, relevance, and firing: a priority map for target selection. Trends in
939 Cognitive Sciences 10:382–390.

940 Feldmann-Wüstefeld T, Schubö A (2016) Intertrial priming due to distractor repetition is eliminated in
941 homogeneous contexts. Atten Percept Psychophys 78:1935–1947.

942 Foster JJ, Bsales EM, Jaffe RJ, Awh E (2017a) Alpha-Band Activity Reveals Spontaneous
943 Representations of Spatial Position in Visual Working Memory. Current Biology 27:3216-3223.e6.

944 Foster JJ, Sutterer DW, Serences JT, Vogel EK, Awh E (2017b) Alpha-Band Oscillations Enable Spatially
945 and Temporally Resolved Tracking of Covert Spatial Attention. Psychological Science 28:929–
946 941.

947 Friston K (2005) A theory of cortical responses. Phil Trans R Soc B 360:815–836.

948 Gandhi SP, Heeger DJ, Boynton GM (1999) Spatial attention affects brain activity in human primary
949 visual cortex. Proceedings of the National Academy of Sciences 96:3314–3319.

950 Gardner JL, Sun P, Waggoner RA, Ueno K, Tanaka K, Cheng K (2005) Contrast Adaptation and
951 Representation in Human Early Visual Cortex. Neuron 47:607–620.

952 Gaspar JM, McDonald JJ (2014) Suppression of Salient Objects Prevents Distraction in Visual Search.
953 Journal of Neuroscience 34:5658–5666.

954 Gaspelin N, Leonard CJ, Luck SJ (2015) Direct Evidence for Active Suppression of Salient-but-Irrelevant
955 Sensory Inputs. Psychol Sci 26:1740–1750.

956 Gaspelin N, Leonard CJ, Luck SJ (2017) Suppression of overt attentional capture by salient-but-irrelevant
957 color singletons. Attention, Perception, & Psychophysics 79:45–62.

958 Gaspelin N, Luck SJ (2018) Distinguishing among potential mechanisms of singleton suppression.
959 Journal of Experimental Psychology: Human Perception and Performance 44:626–644.

960 Geng JJ (2014) Attentional Mechanisms of Distractor Suppression. Curr Dir Psychol Sci 23:147–153.

961 Geng JJ, Won B-Y, Carlisle NB (2019) Distractor Ignoring: Strategies, Learning, and Passive Filtering.
962 Curr Dir Psychol Sci 28:600–606.

963 Geyer T, Müller HJ, Krummenacher J (2006) Cross-trial priming in visual search for singleton conjunction
964 targets: Role of repeated target and distractor features. Perception & Psychophysics 68:736–749.

965 Goschy H, Bakos S, MÃ¼ller HJ, Zehetleitner M (2014) Probability cueing of distractor locations: both
966 intertrial facilitation and statistical learning mediate interference reduction. Front Psychol 5
967 Available at: http://journal.frontiersin.org/article/10.3389/fpsyg.2014.01195/abstract [Accessed
968 September 8, 2020].

969 Greve DN, Fischl B (2009) Accurate and robust brain image alignment using boundary-based registration.
970 NeuroImage 48:63–72.

971 Grill-Spector K, Malach R (2001) fMR-adaptation: a tool for studying the functional properties of human
972 cortical neurons. Acta Psychologica 107:293–321.

973 Haynes J-D, Rees G (2005) Predicting the orientation of invisible stimuli from activity in human primary
974 visual cortex. Nat Neurosci 8:686–691.

975 Heuer A, Schubö A (2019) Cueing distraction: electrophysiological evidence for anticipatory active
976 suppression of distractor location. Psychological Research Available at:
977 http://link.springer.com/10.1007/s00426-019-01211-4 [Accessed September 8, 2020].

978 Hickey C, Di Lollo V, McDonald JJ (2009) Electrophysiological Indices of Target and Distractor
979 Processing in Visual Search. Journal of Cognitive Neuroscience 21:760–775.

980 Hickey C, Peelen MV (2015) Neural Mechanisms of Incentive Salience in Naturalistic Human Vision.
981 Neuron 85:512–518.

982 Hickey C, Peelen MV (2017) Reward Selectively Modulates the Lingering Neural Representation of
983 Recently Attended Objects in Natural Scenes. J Neurosci 37:7297–7304.

984 Hupé JM, James AC, Payne BR, Lomber SG, Girard P, Bullier J (1998) Cortical feedback improves
985 discrimination between figure and background by V1, V2 and V3 neurons. Nature 394:784–787.

986 Ipata AE, Gee AL, Bisley JW, Goldberg ME (2009) Neurons in the lateral intraparietal area create a
987 priority map by the combination of disparate signals. Experimental Brain Research 192:479–488.

988 Ipata AE, Gee AL, Gottlieb J, Bisley JW, Goldberg ME (2006) LIP responses to a popout stimulus are
989 reduced if it is overtly ignored. Nature Neuroscience 9:1071–1076.

990 Itthipuripat S, Vo VA, Sprague TC, Serences JT (2019) Value-driven attentional capture enhances
991 distractor representations in early visual cortex Tong F, ed. PLoS Biol 17:e3000186.

992 Itti L, Koch C (2000) A saliency-based search mechanism for overt and covert shifts of visual attention.
993 Vision Research 40:1489–1506.

994 Jehee JFM, Ling S, Swisher JD, van Bergen RS, Tong F (2012) Perceptual Learning Selectively Refines
995 Orientation Representations in Early Visual Cortex. Journal of Neuroscience 32:16747–16753.

996 Jenkinson M, Bannister P, Brady M, Smith S (2002) Improved Optimization for the Robust and Accurate
997 Linear Registration and Motion Correction of Brain Images. NeuroImage 17:825–841.

998 Jenkinson M, Beckmann CF, Behrens TEJ, Woolrich MW, Smith SM (2012) FSL. NeuroImage 62:782–
999 790.

1000 Jenkinson M, Smith S (2001) A global optimisation method for robust affine registration of brain images.
1001 Medical Image Analysis 5:143–156.

1002 Kamitani Y, Tong F (2005) Decoding the visual and subjective contents of the human brain. Nat Neurosci
1003 8:679–685.

1004 Karni A, Sagi D (1991) Where practice makes perfect in texture discrimination: evidence for primary visual
1005 cortex plasticity. Proceedings of the National Academy of Sciences 88:4966–4970.

1006 Kastner S (1998) Mechanisms of Directed Attention in the Human Extrastriate Cortex as Revealed by
1007 Functional MRI. Science 282:108–111.

1008 Kastner S, Pinsk MA, De Weerd P, Desimone R, Ungerleider LG (1999) Increased Activity in Human
1009 Visual Cortex during Directed Attention in the Absence of Visual Stimulation. Neuron 22:751–761.

1010 Kastner S, Ungerleider LG (2000) Mechanisms of Visual Attention in the Human Cortex. Annu Rev
1011 Neurosci 23:315–341.

1012 Kim H, Anderson BA (2019) Dissociable neural mechanisms underlie value-driven and selection-driven
1013 attentional capture. Brain Research 1708:109–115.

1014 Kristjansson A, Vuilleumier P, Schwartz S, Macaluso E, Driver J (2007) Neural Basis for Priming of Pop-
1015 Out during Visual Search Revealed with fMRI. Cerebral Cortex 17:1612–1624.

1016 Lawson CL, Hanson RJ (1974) Chapter 23. In: Solving Least-Squares Problems. Upper Saddle River,
1017 New Jersey: Prentice-Hall.

1018 Le Pelley ME, Mitchell CJ, Beesley T, George DN, Wills AJ (2016) Attention and associative learning in
1019 humans: An integrative review. Psychological Bulletin 142:1111–1140.

1020 Lewis-Peacock JA, Postle BR (2012) Decoding the internal focus of attention. Neuropsychologia 50:470–
1021 478.

1022 Li Z (2002) A saliency map in primary visual cortex. Trends in Cognitive Sciences 6:9–16.

1023 Luck SJ, Chelazzi L, Hillyard SA, Desimone R (1997) Neural Mechanisms of Spatial Selective Attention in
1024 Areas V1, V2, and V4 of Macaque Visual Cortex. Journal of Neurophysiology 77:24–42.

1025 MacLean MH, Giesbrecht B (2015) Neural evidence reveals the rapid effects of reward history on
1026 selective attention. Brain Research 1606:86–94.

1027 Maljkovic V, Nakayama K (1994) Priming of pop-out: I. Role of features. Memory & Cognition 22:657–
1028 672.

1029 Maunsell JHR (2004) Neuronal representations of cognitive state: reward or attention? Trends in
1030 Cognitive Sciences 8:261–265.

1031 Mazer JA, Gallant JL (2003) Goal-Related Activity in V4 during Free Viewing Visual Search. Neuron
1032 40:1241–1250.

1033 Moher J, Egeth HE (2012) The ignoring paradox: Cueing distractor features leads first to selection, then
1034 to inhibition of to-be-ignored items. Attention, Perception, & Psychophysics 74:1590–1605.

1035 Moher J, Lakshmanan BM, Egeth HE, Ewen JB (2014) Inhibition Drives Early Feature-Based Attention.
1036 Psychological Science 25:315–324.

1037 Mostert P, Albers AM, Brinkman L, Todorova L, Kok P, de Lange FP (2018) Eye Movement-Related
1038 Confounds in Neural Decoding of Visual Working Memory Representations. eNeuro
1039 5:ENEURO.0401-17.2018.

1040 Motter BC (1993) Focal attention produces spatially selective processing in visual cortical areas V1, V2,
1041 and V4 in the presence of competing stimuli. Journal of Neurophysiology 70:909–919.

1042 Mounts JRW (2000) Evidence for suppressive mechanisms in attentional selection: Feature singletons
1043 produce inhibitory surrounds. Perception & Psychophysics 62:969–983.

1044 Norman KA, Polyn SM, Detre GJ, Haxby JV (2006) Beyond mind-reading: multi-voxel pattern analysis of
1045 fMRI data. Trends in Cognitive Sciences 10:424–430.

1046 Ogawa T, Komatsu H (2006) Neuronal dynamics of bottom-up and top-down processes in area V4 of
1047 macaque monkeys performing a visual search. Exp Brain Res 173:1–13.

1048 Olivers CNL, Meijer F, Theeuwes J (2006) Feature-based memory-driven attentional capture: Visual
1049 working memory content affects visual attention. Journal of Experimental Psychology: Human
1050 Perception and Performance 32:1243–1265.

1051 Pashler H, Shiu L (1999) Do images involuntarily trigger search? A test of Pillsbury's hypothesis.
1052 Psychonomic Bulletin & Review 6:445–448.

1053 Pelli DG (1997) The VideoToolbox software for visual psychophysics: transforming numbers into movies.
1054 Spatial Vision 10:437–442.

1055 Poltoratski S, Ling S, McCormack D, Tong F (2017) Characterizing the effects of feature salience and top-
1056 down attention in the early visual system. Journal of Neurophysiology 118:564–573.

1057 Rademaker RL, Chunharas C, Serences JT (2019) Coexisting representations of sensory and mnemonic
1058 information in human visual cortex. Nat Neurosci 22:1336–1344.

1059 Rao RPN, Ballard DH (1999) Predictive coding in the visual cortex: a functional interpretation of some
1060 extra-classical receptive-field effects. Nat Neurosci 2:79–87.

1061 Reavis EA, Frank SM, Greenlee MW, Tse PU (2016) Neural correlates of context-dependent feature
1062 conjunction learning in visual search tasks. Hum Brain Mapp 37:2319–2330.

1063 Reeder RR, Olivers CNL, Pollmann S (2017) Cortical evidence for negative search templates. Visual
1064 Cognition 25:278–290.

1065 Rungratsameetaweemana N, Serences JT (2019) Dissociating the impact of attention and expectation on
1066 early sensory processing. Current Opinion in Psychology 29:181–186.

1067 Saproo S, Serences JT (2010) Spatial Attention Improves the Quality of Population Codes in Human
1068 Visual Cortex. Journal of Neurophysiology 104:885–895.

1069 Sawaki R, Luck SJ (2010) Capture versus suppression of attention by salient singletons:
1070 Electrophysiological evidence for an automatic attend-to-me signal. Attention, Perception, &
1071 Psychophysics 72:1455–1470.

1072 Schwartz S, Maquet P, Frith C (2002) Neural correlates of perceptual learning: A functional MRI study of
1073 visual texture discrimination. Proceedings of the National Academy of Sciences 99:17137–17142.

1074 Serences JT (2008) Value-Based Modulations in Human Visual Cortex. Neuron 60:1169–1181.

1075 Serences JT, Saproo S (2012) Computational advances towards linking BOLD and behavior.
1076 Neuropsychologia 50:435–446.

1077 Serences JT, Yantis S (2006) Selective visual attention and perceptual coherence. Trends in Cognitive
1078 Sciences 10:38–45.

1079 Serences JT, Yantis S (2007) Spatially Selective Representations of Voluntary and Stimulus-Driven
1080 Attentional Priority in Human Occipital, Parietal, and Frontal Cortex. Cerebral Cortex 17:284–293.

1081 Serences JT, Yantis S, Culberson A, Awh E (2004) Preparatory Activity in Visual Cortex Indexes
1082 Distractor Suppression During Covert Spatial Orienting. Journal of Neurophysiology 92:3538–
1083 3545.

1084 Silver MA, Ress D, Heeger DJ (2005) Topographic Maps of Visual Spatial Attention in Human Parietal
1085 Cortex. Journal of Neurophysiology 94:1358–1371.

1086 Smith SM, Jenkinson M, Woolrich MW, Beckmann CF, Behrens TEJ, Johansen-Berg H, Bannister PR,
1087 De Luca M, Drobnjak I, Flitney DE, Niazy RK, Saunders J, Vickers J, Zhang Y, De Stefano N,
1088 Brady JM, Matthews PM (2004) Advances in functional and structural MR image analysis and
1089 implementation as FSL. NeuroImage 23:S208–S219.

1090 Solomon SG, Kohn A (2014) Moving Sensory Adaptation beyond Suppressive Effects in Single Neurons.
1091 Current Biology 24:R1012–R1022.

1092 Somers DC, Dale AM, Seiffert AE, Tootell RBH (1999) Functional MRI reveals spatially specific
1093 attentional modulation in human primary visual cortex. Proceedings of the National Academy of
1094 Sciences 96:1663–1668.

1095 Soto D, Heinke D, Humphreys GW, Blanco MJ (2005) Early, Involuntary Top-Down Guidance of Attention
1096 From Working Memory. Journal of Experimental Psychology: Human Perception and
1097 Performance 31:248–261.

1098 Sprague TC, Adam KCS, Foster JJ, Rahmati M, Sutterer DW, Vo VA (2018a) Inverted Encoding Models
1099 Assay Population-Level Stimulus Representations, Not Single-Unit Neural Tuning. eNeuro
1100 5:ENEURO.0098-18.2018.

1101 Sprague TC, Boynton GM, Serences JT (2019) The Importance of Considering Model Choices When
1102 Interpreting Results in Computational Neuroimaging. eNeuro 6:ENEURO.0196-19.2019.

1103 Sprague TC, Itthipuripat S, Vo VA, Serences JT (2018b) Dissociable signatures of visual salience and
1104 behavioral relevance across attentional priority maps in human cortex. Journal of
1105 Neurophysiology Available at: http://www.physiology.org/doi/10.1152/jn.00059.2018 [Accessed
1106 March 20, 2018].

1107 Sprague TC, Serences JT (2013) Attention modulates spatial priority maps in the human occipital,
1108 parietal and frontal cortices. Nature Neuroscience 16:1879–1887.

1109 Spratling MW (2008) Predictive coding as a model of biased competition in visual attention. Vision
1110 Research 48:1391–1408.

1111 Spratling MW (2017) A review of predictive coding algorithms. Brain and Cognition 112:92–97.

1112 Srinivasan MV, Laughlin SB, Dubs A (1982) Predictive coding: a fresh view of inhibition in the retina. Proc
1113 R Soc Lond B 216:427–459.

1114 Stanisor L, van der Togt C, Pennartz CMA, Roelfsema PR (2013) A unified selection signal for attention
1115 and reward in primary visual cortex. Proceedings of the National Academy of Sciences
1116 110:9136–9141.

1117 Summerfield C, de Lange FP (2014) Expectation in perceptual decision making: neural and
1118 computational mechanisms. Nat Rev Neurosci 15:745–756.

1119 Swisher JD, Halko MA, Merabet LB, McMains SA, Somers DC (2007) Visual Topography of Human
1120 Intraparietal Sulcus. Journal of Neuroscience 27:5326–5337.

1121 Theeuwes J (1992) Perceptual selectivity for color and form. Perception & Psychophysics 51:599–606.

1122 Theeuwes J (2019) Goal-driven, stimulus-driven, and history-driven selection. Current Opinion in
1123 Psychology 29:97–101.

1124 Tong F, Pratte MS (2012) Decoding Patterns of Human Brain Activity. Annu Rev Psychol 63:483–509.

1125 Tootell RBH, Hadjikhani N, Hall EK, Marrett S, Vanduffel W, Vaughan JT, Dale AM (1998) The Retinotopy
1126 of Visual Spatial Attention. Neuron 21:1409–1422.

1127 Treisman AM, Gelade G (1980) A feature-integration theory of attention. Cognitive Psychology 12:97–
1128 136.

Turatto M, Bonetti F, Pascucci D, Chelazzi L (2018) Desensitizing the attention system to distraction while idling: A new latent learning phenomenon in the visual attention domain. Journal of Experimental Psychology: General 147:1827–1850.

Turatto M, Galfano G (2001) Attentional capture by color without any relevant attentional set. Perception & Psychophysics 63:286–297.

Turatto M, Pascucci D (2016) Short-term and long-term plasticity in the visual-attention system: Evidence from habituation of attentional capture. Neurobiology of Learning and Memory 130:159–169.

van Bergen RS, Jehee JFM (2019) Probabilistic Representation in Human Visual Cortex Reflects Uncertainty in Serial Decisions. J Neurosci 39:8164–8176.

van Bergen RS, Ji Ma W, Pratte MS, Jehee JFM (2015) Sensory uncertainty decoded from visual cortex predicts behavior. Nat Neurosci 18:1728–1730.

Van Moorselaar D, Slagter HA (2020) Inhibition in selective attention. Annals of the New York Academy of Sciences 1464:204–221.

Vatterott DB, Vecera SP (2012) Experience-dependent attentional tuning of distractor rejection. Psychon Bull Rev 19:871–878.

Wang B, Theeuwes J (2018a) Statistical regularities modulate attentional capture. Journal of Experimental Psychology: Human Perception and Performance 44:13–17.

Wang B, Theeuwes J (2018b) How to inhibit a distractor location? Statistical learning versus active, top-down suppression. Attention, Perception, & Psychophysics Available at: http://link.springer.com/10.3758/s13414-018-1493-z [Accessed March 20, 2018].

Westerberg JA, Cox MA, Dougherty K, Maier A (2019) V1 microcircuit dynamics: altered signal propagation suggests intracortical origins for adaptation in response to visual repetition. Journal of Neurophysiology 121:1938–1952.

Wolfe JM (1994) Guided Search 2.0 A revised model of visual search. Psychonomic Bulletin & Review 1:202–238.

Won B-Y, Forloines M, Zhou Z, Geng JJ (2020) Changes in visual cortical processing attenuate singleton distraction during visual search. Cortex 132:309–321.

Won B-Y, Geng JJ (2020) Passive exposure attenuates distraction during visual search. Journal of Experimental Psychology: General Available at: http://doi.apa.org/getdoi.cfm?doi=10.1037/xge0000760 [Accessed June 15, 2020].

Zhang W, Luck SJ (2009) Feature-based attention modulates feedforward visual processing. Nat Neurosci 12:24–25.

Zhang X, Zhaoping L, Zhou T, Fang F (2012) Neural Activities in V1 Create a Bottom-Up Saliency Map. Neuron 73:183–192.